The Pennsylvania State University

The Graduate School

A THESIS IN EVALUATING THE IMPACT OF A CONSTRUCTED FLOODPLAIN WETLAND ON WATER QUALITY IN AN URBAN STREAM IN STATE COLLEGE, PA

A Thesis in

Environmental Engineering

by

Liyan Fan

Submission in Partial Fulfillment

of the Requirements

for the Degree of

Master of Science

August 2021

The thesis of Liyan Fan was reviewed and approved by the following:

Lauren McPhillips,
Assistant Professor of Civil and Environmental Engineering
Thesis Advisor

Li Li,
Associate Professor of Civil and Environmental Engineering

Nathaniel Warner,
Assistant Professor of Civil and Environmental Engineering

Patrick Fox,
Professor of Civil and Environmental Engineering
Head of the Department of Civil and Environmental Engineering

Abstract

This thesis is focused on evaluating water quality function of a constructed floodplain wetland located along an urban stream in State College, Pennsylvania. Analysis of hydrology as well as nitrogen, phosphorous, and sediment patterns from baseflow and stormwater samples are presented from multiple sites in the wetland and adjacent urban stream. The data demonstrates that the wetland provides reduction in nitrogen and sediments when it receives water during baseflow periods, but no reduction for phosphorous. During storm events, sediment (28~99 %) and phosphorous (11~91%) removal ratios in the wetland are high while nitrogen removal is decent(-16~47 %). The wetland also has the function of stormwater runoff removal (17~57%). The wetland has good nitrogen removal efficiency during P-limitation time and good Phosphorous removal efficiency during N-limitation time. Thus, when evaluating effectiveness of the constructed floodplain wetland as an individual unit, it performs well for nutrient and sediment removal. However, given that the amount of water diverted from the stream to the wetland is often between 1-5% of streamflow, depending on the magnitude of streamflow, the wetland's impact on the adjacent stream is low. It's recommended to adjust inlet design to increase the amount of water entering into the wetland.

Table of Contents

Acknowledgements

I sincerely appreciate the work of the spring 2019 CE/ABE 597 class in Urban Hydrology and Biogeochemistry which collected some initial data and information on Walnut Run as part of a class project. I also appreciate field assistance from Maria Iglesias Thome, Xunheng Xu, Jace Marsh and Jeff Zaengle. I thank the Penn State EESL Green student award for water quality analysis of TP. I also thank the College of Agricultural Sciences Undergraduate Research Award for a summer grant to Maria Iglesias, Thome and Xunheng Xu that supported additional research at Walnut Run.

Introduction

Pollutants In Chesapeake Bay

Pollutants in water bodies can cause severe environmental and health problems, such as eutrophication. It can destroy water ecosystems and lead to human diseases such as rashes, respiratory illness and neuro illness because of toxicity of algae (US EPA, 2013). One byproduct of water treatment to eutrophic water is dioxin, a critical carcinogen agent (US EPA, 2013). Algae also blocks light and oxygen and create a 'dead zone' in water bodies in which living organisms cannot grow or breathe. The 'dead zone', or hyoxia zone, is defined as regions that dissolved oxygen (DO) is below 2mg/L (Testa et al., 2017). (Tian, 2020) shows that most serious hypoxia happens in July, with around $8*10^7$ m^3 hypoxia volume in Chesapeake Bay, which is 0.12% of total water volume (68 billion m^3, (Facts & Figures | Chesapeake Bay Program, 2017) in Chesapeake Bay.

Chesapeake Bay is the largest estuary in United States, whose watershed (approximately 165,800 km^2) (Fanelli et al., 2019) spans Delaware, Maryland, New York, Pennsylvania, Virginia, West Virginia, and the District of Columbia, with over 150 tributaries (DeLuca et al., 2018) and 18 million watershed residents (Testa et al., 2017). Chesapeake Bay is experiencing serious nutrient and sediment problems. (Harding et al., 2020) states the Chesapeake Bay is eutrophic with 301-500 g C m^{-2} y^{-1} annual phytoplankton primary production . Chloroplast concentration and net primary production increased in all water bodies in the Bay from 1985-2005, except a slight decrease of net primary production in high salinity (polyhaline) water. The US Environmental Protection Agency (EPA) has set regulations that the Total Daily Maximum Load for Total Dissolved Nitrogen (TDN), Total Phosphorous (TP) and Total Suspended Solid (TSS) contributions should be decreased by 25%, 24% and 20% respectively due to the worsening water quality in Chesapeake Bay (R. 03 US EPA, 2015). Pennsylvania is defined as largest source of nitrogen, second largest source of phosphorus, sediment and industrial wastewater load among the states of Chesapeake Bay watershed (*Section 4. Sources of Nitrogen, Phosphorus and Sediment to the Chesapeake Bay*, 2010). The most important sources of pollutants in PA for Chesapeake Bay are agriculture and forest. Decreasing agriculture land and forest, failure in implementing Agricultural Compliance and Enforcement Strategy, undersized and aging sewer system and increasing vehicles causes failure for PA to achieve 2025 Clean Water Blueprint Goals (*Pennsylvania's Blueprint for Clean Water*, 2021).

In addition, there are explicit flushing patterns for nutrients and sediments in the Chesapeake Bay in the past 30 years. Flushing patterns means thigher concentration of pollutants occurs in high flow time rather than low flow time. (Zhang, 2018) shows that the flushing pattern for TP is increasing from 1985 to 2015 during high flow times. Increasing flushing trends of PO_4 happen in multiple tributaries of the Bay (Fanelli et al., 2019).

Understanding sources and impacts of pollutants

Nitrogen (N) and phosphorus (P) are main sources of eutrophication. Algae bloom significantly increases only when both N and P concentrations are high (Dodds & Smith, 2016). The mainstem of Chesapeake Bay is changing nutrient limitation type from P-limitation to N limitation because of effectiveness in N removal in wastewater treatment and Clean Air Act that decrease N emission (Zhang et al., 2021). Obvious N-limitation happens in dry seasons as there are little untreated freshwater input.

TDNis composed of Particulate Nitrogen as well as Total Dissolved Nitrogen (TDN), which includes ammonium (NH_4^+), nitrate (NO_3^-), nitrite (NO_2-) and dissolved organic-bound nitrogen (*Total Nitrogen in Wastewater*, 2013). Dissolved forms of nitrogen are particularly of interest given that they are most biologically available, and thus contribute most directly to eutrophication. Although NH_4^+ is relatively unregulated and increased 11% in 1990-2010 (Campbell et al., 2019), the portion of NH_4^+ in watersheds is only around 1% (Ludwig, 2010). The main sources of nitrogen are agriculture (50%), sewage (25%), atmospheric deposition (15%), urban stormwater (5%), and septic systems (3%) (Shenk & Linker, 2013). Point sources (sewage, urban stormwater and septic) decreased significantly in 1992-2012 (Ator et al., 2019).

TP includes soluble phosphorus (mainly phosphate) and particulate phosphorus (mainly dimple phosphomonoesters, phosphodiesters, inositol phosphate) (Steidinger et al., 2015). Phosphorus is often associated with sediment through sorption or mineral complexes. Sources of TP in Chesapeake Bay are mainly from agriculture (40%), industrial wastewater (30%), forest (15%), and urban stormwater (10%), among which agriculture and mineral source slightly increased in 1992-2012 (Ator et al., 2019; Shenk & Linker, 2013). Phosphorus is worth investigating because phosphorus is usually limiting nutrients for crops and aquatic autotrophs (Ludwig, 2010), so it should be prevented from being washed away and contributing to downstream eutrophication.

TSS is the dry weight of all the particles that not dissolved in water. 69% mass of TSS comes from agriculture land, 15% of TSS comes from urban wastewater and forest each (Son & Wang, 2012). Sediments are of concern because they depress seed emergence and decline crop yield (Son & Wang, 2012). They also block light and other radiation for submerged aquatic plant growth (DeLuca et al., 2018; Son & Wang, 2012). Sediments can also improve pathogenic bacteria growth in water because the bacteria reside in water by attach to suspended sediments (Davis et al., 2017; DeLuca et al., 2018). Therefore, sediments play a two-way role in nutrient assimilation- small amounts of sediments promote the growth of microorganisms, thus promoting microorganisms' absorption of nutrients; excessive sediment blocks light and oxygen and depress microorganisms' absorption of nutrients (Foladori et al., 2020).

Best Management Practices for Nutrient and Sediment Management

In order to prevent these negative impacts of nutrients and sediments on downstream waters, Best Management Practices (BMPs) are implemented. BMPs can be structural or nonstructural features that reduce inputs and/or retain and transform nutrients and sediment. There are many types of structural BMPs that may be located up in the watershed near where runoff is generated, or near to streams. Type of BMP may also vary depending on the type of land use such as agriculture or urban development(Liu et al., 2017). Examples of structural BMPs include detention basins, bioretention cells, filter strips, green roof, riparian buffers, constructed wetlands, and stream restoration(Clary et al., 2020; Liu et al., 2017; Xu et al., 2017). There is a large body of work dedicated to understanding the effectiveness of BMPs at the site scale and watershed scale . Different types of BMPs have different advantages--green roof has relatively good capacity of TDN removal and runoff reduction, bioretention systems are good at metal and TSS removal, dry detention basins are good at TSS removal(Liu et al., 2017).It is critical to understand what factors influence this variability, in order to design more effective BMPs (Clary et al., 2020; Xu et al., 2017). In this article the focus is a relatively understudied type of BMP, constructed floodplain wetlands.

Constructed Wetlands

Wetlands are defined as areas that contain hydric soils, wetland vegetation, and are ponded or saturated by surface or ground water either permanently or seasonally (Ludwig, 2010). Water and vegetation in wetlands are able to support life in saturated and anoxic conditions (Keddy, 2010; Ludwig, 2010). Floodplain wetlands are wetlands that are part of the floodplain, which are transition zones between a stream or river and upslope areas (Keeter, 2019; Ludwig, 2010; Yin et al., 2019). Floodplains have abundant wetland vegetation, low slope gradients, and high material transfer rate between water body and surrounding terrains, which makes them efficient for facilitating attenuation of flood peaks and nutrient and sediment retention and an ideal place for a constructed wetland (A. L. Ludwig & Hession, 2015; Yin et al., 2019).

Constructed wetlands are engineered systems that have been designed and constructed to simulate soils, vegetations, nutrient assimilation and microbial processes in natural wetlands (Andrea Lorene Ludwig, 2010; Vymazal, 2010). Constructed wetlands can be categorized into free water surface wetlands, horizontal flow wetlands, and vertical flow wetlands based on flow direction (A. L. Ludwig, 2010; Resende et al., 2019). The mechanisms of pollutant removal in constructed wetlands are physical processes (adsorption, volatilization, debris filtration), chemical processes (sedimentation, complexation) and biological uptake via vegetation or microbes (Birch et al., 2004; O'Shea et al., 1999). Constructed wetlands have been implemented as water quality BMPs due to their strong pollutant removal capabilities, low efficiency decay rate and easy management and maintenance (O'Shea et al., 1999; Resende et al., 2019). They have extraordinary removal efficiency of TP and above-average removal efficiency of TDN and TSS compared to other types of BMPs (Clary et al., 2020). However, constructed wetlands implemented in stream floodplains have not been a commonly implemented type of BMP; more often constructed wetlands are located further up in watersheds near sources of runoff/polluted water generation. Given their potential to contribute to nutrient and sediment retention, and aid in reaching Chesapeake Bay water quality goals, there is a need for understanding the potential benefits of constructed floodplain wetlands as a BMP in this region.

Objectives

The objectives of this thesis are:

1. Characterize nutrient and sediment sources to an urban stream and constructed floodplain wetland with synoptic surveys
2. Characterize stream and wetland hydrology
3. Quantify sediment and nutrient removal efficiency of the wetland under baseflow and stormflow conditions
4. Evaluate the potential impact of the wetland on stream water quality

Methods

Site Description

Walnut Run is a highly urbanized stream located in State College Borough in central Pennsylvania (**Figure 1**). The stream is a part of the Spring Creek and Chesapeake Bay watershed (Run, 2013). This urban stream has the potential to affect downstream hydrology and water quality through increasing peak flows, flow rate, nutrient transport, and salinity. Sources of water to the stream include both urban stormwater as well as groundwater. The most upstream portion of the stream has been buried underground into the storm sewer system. The stream 'daylights' at University Ave, at the edge of Walnut Springs Park. Walnut Spring enters the stream several hundred meters into the park and provides much of Walnut Run's baseflow and has the potential to contribute substantial nutrient loads from the legacy of agriculture on regional groundwater nutrient concentrations. However, there is a limited understanding of nutrient and sediment dynamics along the stream.

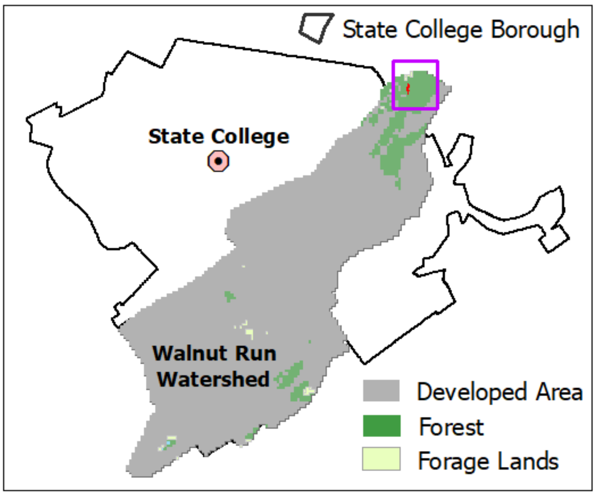

Figure 1. Map of Walnut Run watershed and predominant land cover, with the study extent

within Walnut Springs Park highlighted in purple

In Walnut Springs Park, there is a constructed floodplain wetland that was installed in 2005 to mitigate both stream discharge patterns and nutrient and sediment loads (**Figure 2**). The wetland has two inflow/ diversion points from the stream (**Figure 3**) located within several meters of each other, as well as one outflow point from the wetland to the stream (**Figure 4**). Both the pipe inflow and outflow points also have control boxes, where the inflow box is generally set to permit maximum inflow, and the outflow box is generally set to permit minimum outflow (or maximum retention). While not all original design details have been able to be obtained from State College Borough or the original designer (Skelly and Loy), basic details are shown in **Figure 2**. The primary flow path through the wetland is approximately 75 meters long.

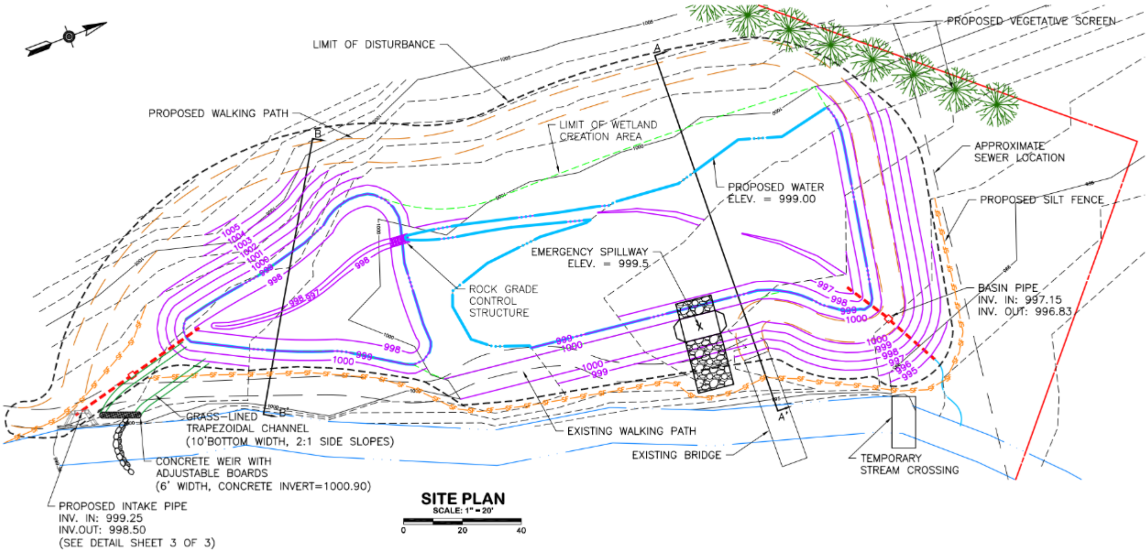

Figure 2. Original proposed design plan for constructed floodplain wetland (Source; Skelly and Loy/ State College Borough)

Figure 3. Locations along stream where water is diverted into wetland, including a wooden slatted weir (left) and a pipe (right)

Figure 4. Outflow pipe from wetland to stream. A Thel-Mar pipe weir is shown, which was used to facilitate water level and discharge monitoring.

Sampling Methods

1. Water level and discharge monitoring

In order to understand the hydrologic dynamics of the stream and wetland, water level was monitored continuously in the stream, both upstream and downstream of the wetland, as well as at the inflow and outflow points to the wetland (**Figure 5**). The data record analyzed is from 2020/3/10-2021/3/18. The water level was measured by a pressure transducer connected to an ISCO 6712C automated sampler (**Figure 6**) and the data can be automatically recorded at 10-minute intervals and downloaded to a computer. Those water level data were converted to discharge (volumetric flow rate) data by rating curve. While the upstream, downstream, and inflow pressure transducers were mounted directly on the stream or wetland sediment using an anchoring device, the wetland outflow pipe was instrumented with a 12-inch Thel-Mar pipe weir, behind which the pressure transducer was located.

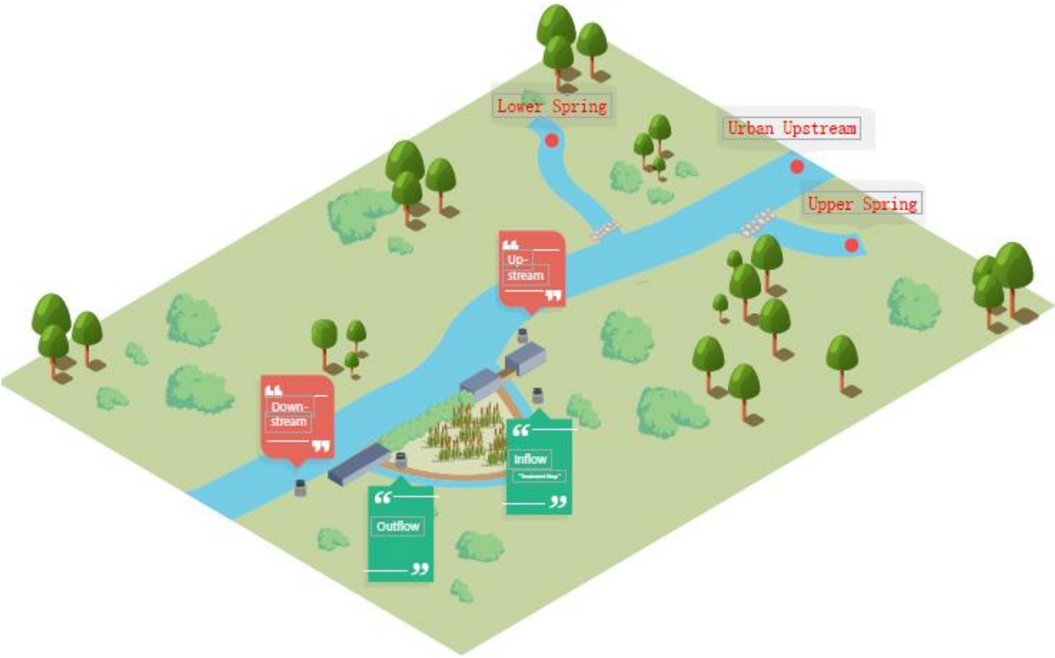

Figure 5. Sampling locations for synoptic sampling events along entire stream and continuous water level monitoring/ storm sampling (upstream, inflow, outflow, downstream sites)

Figure 6. ISCO Sampler with computer used to download data

We use the 'Area-Velocity' approach for discharge measurement, which means integrating the product of area and velocity of each segment of a cross section (**Figure 6**) (*How Streamflow Is Measured*, 2021). Velocity was measured at multiple points at a given cross-section using a Marsh-McBirney electromagnetic flow meter. The discharge should be measured at each site of Walnut Run during a range of flow conditions every season to make a precise rating curve to relate water level to discharge. The rating curve is used to convert water level timeseries into consecutive discharge data in time series. A weir rating curve obtained from the pipe weir manufacturer (Thel-Mar) was used to convert outflow water levels to discharge values. Verification was provided using multiple manual measurements of volumetric flow rate from the pipe.

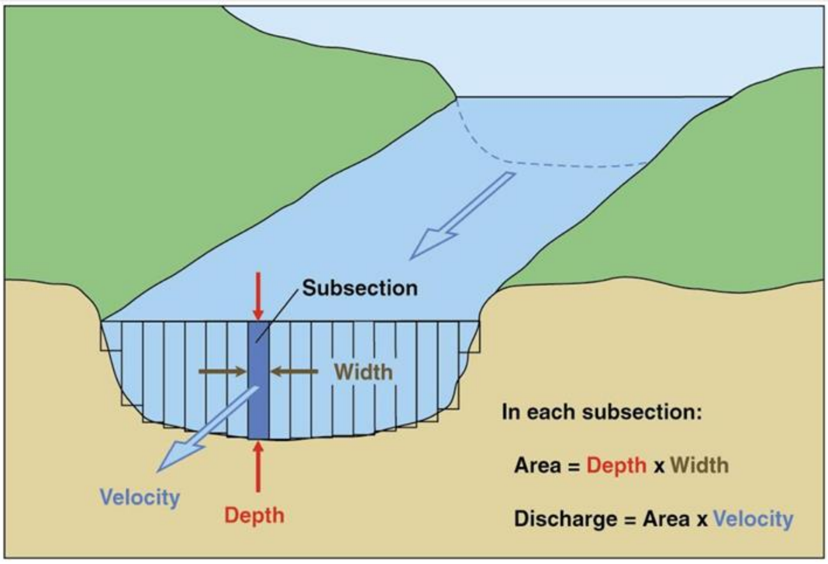

Figure 7. Schematic of area-velocity method of discharge measurement (Source: USGS)

3. Storm sampling

The ISCO samplers were applied in storm sampling. They were set to trigger with a 2 cm increase in water level in 15 min. The ISCO sampler only starts to collect water sample when the water level increase is greater than or equal to the trigger level. Prior to a target storm event, ice was added to the sample carousel to maintain the integrity of the samples until they could be retrieved. The 500 ml ISCO bottle was filled every 20 minutes. The sampling process ends when all the 24 bottles in the ISCO sampler tray have been filled. In one longer storm event, the first bottles were replaced with empty ones to allow us to capture the entire event. Four storm events were sampled: 7/9/20, 9/2/20, 11/11/20, and 3/18/21.

4. Synoptic baseflow sampling

To complement the storm sampling, and better characterize upstream sources of nutrients and sediments, we also performed synoptic sampling along the stream and wetland during baseflow periods. The section of stream evaluated begins after the stream daylights in Walnut Spring Park and continues to just below the wetland (**Figure 5**). These eight sampling events span 2019 through 2020. Baseflow sampling opportunities were limited in 2020 due to the regional drought that caused water levels to consistently remain below the wetland inflow pipe, except during and directly following storm events.

For this sampling, each site in **Figure 5** was visited. Samples were collected upstream of wetland, at wetland inflow, wetland outflow, and downstream of wetland, as well as at the upper Walnut spring, a second lower spring, and the urban channel upstream of the Walnut

Spring. A 1L polyethylene bottle was filled with water from the middle of the stream/water source at the middle depth of water column.

5. Lab Methods

All of the water samples (including storm samples and non-storm baseflow samples) were kept at 4°C in a refrigerator and were processed within several days of sampling. Total suspended solids (TSS), Cl^-,NO_3^-, total dissolved nitrogen (TDN), and total phosphorus (TP) were the properties of water samples that needed to be measured in the lab. All samples were processed in the Kappe Environmental Engineering Labs.

TSS is measured by filtering the water sample using a 934-AH glass fiber filter. Suspended solid will remain on filter paper after filtering. After drying the filter, we can get the mass of TSS by comparing the filter paper as

$$TSS\left(\frac{mass}{vol}\right) = \frac{dried\ filter\ mass\ with\ suspended\ solids\ - clean\ filter\ mass}{Volume\ of\ filtered\ sample} \quad (1)$$

We used a Dionex ion chromatograph to process Cl^- and NO_3^- for measurement. Filtered water samples processed with 0.45 μm cellulose ester filters are used in this measurement. We used the Shimadzu TOC-V and TNM-1 analyzer for TDN measurement. A filtered water sample is also used in this measurement. TP was measured in the Penn State Energy and Environmental Sustainability Laboratory (EESL) Water Quality Lab via SEAL AQ2 Automated Advanced Discrete Analyzer. Unfiltered water sample is used in this measurement.

Data Analysis

1. Water level, discharge and total volume

The measured discharge data is paired with water level data of that exact measuring time and create rating curve. The rating curve is used to convert water level data in time series into consecutive discharge data in that time series. There should be an individual rating curve for each site.

Then total volume in a specific time period (e.g., during a storm event) can be calculated by summing up products of discharge data (Q) in 10 min time interval and time interval of water level data during that time period (t):

$$Total\ Volume = \sum_{i=1}^{n} Qt \quad (2)$$

2. Water quality concentrations and loads

For each storm event captured, loads of each pollutant in each site is calculated by summing up products of discharge data (Q) in 10 min time interval, measured or interpolated pollutant concentration (c) in the 10 min time interval and time interval of water level data during that time period (t=10min):

$$Total\ Load = \sum_{i=1}^{n} Qct \quad (3)$$

We will calculate ratios between total loads in different sites for each individual pollutant in each event.

3. Water Diversion vs. Precipitation events

Correlation between the ratio of the volume of water diverted into the wetland and the size of the storm event reflects patterns of water entering into wetland and the ability of the wetland to make an impact on downstream water quality. Total water volume of each storm event during 2020/3/10-2021/3/18 will be calculated for the wetland and stream. The ratio of event water volume diverted into the wetland (wetland inflow ratio), precipitation depth (*Climate Information*), precipitation intensity, time duration of storm event in outflow, time duration of the storm event at the downstream site and event duration ratio is recoded for each storm event:

$$\text{Wetland inflow ratio} = \frac{Total\ volume\ of\ storm\ event\ in\ outflow\ (L)}{Total\ volume\ of\ storm\ event\ in\ downstream\ (L)} \quad (4)$$

$$Precipitation\ intensity\ (\frac{inch}{\text{min}}) = \frac{Precipitation\ Depth\ (inch)}{\text{event duration in downstream (min)}} \quad (5)$$

$$Event\ duration\ ratio = \frac{\text{event duration in outflow (min)}}{\text{event duration in downstream (min)}} \quad (6)$$

Event duration was calculated by end time minus start time of an event. The start and time of a storm event in outflow was determined by first and last tim thatquick flow discharge larger than 0.002 m^3/s, as 0.002 m^3/s is the least quick flow (calculated by total flow minus base flow) that can necessarily trigger a water level change detected by ISCO sensor. Quick flow was calculated by baseflow separation using 'EcoHydRology' package in R (**Appendix A**). Time durations of downstream storm events were the times that there is positive discharge. There was no outflow baseflow discharge during the monitored events, and thus separation was not needed.

Results

Baseflow Synoptic Sampling

Synoptic sampling during baseflow periods demonstrates that the most upstream portion of the stream within Walnut Springs Park has relatively low TDN (less than 1 mg L^{-1}; **Figure 8a.**). The Upper (Walnut) Spring and Lower Spring TDN concentrations are much higher (2.5- 4 mg L^{-1}), indicating that these springs are substantial contributors of nitrogen to the stream. Additionally, there were reductions in TDN concentrations between the wetland inflow and outflow points (2-26% reduction). TP and TSS patterns along the stream and wetland during baseflow periods demonstrated minimal differences between sites (**Figure 8b. and c.**). Both TP and TSS had slightly higher concentrations at the wetland inflow as compared to the upstream sampling location.

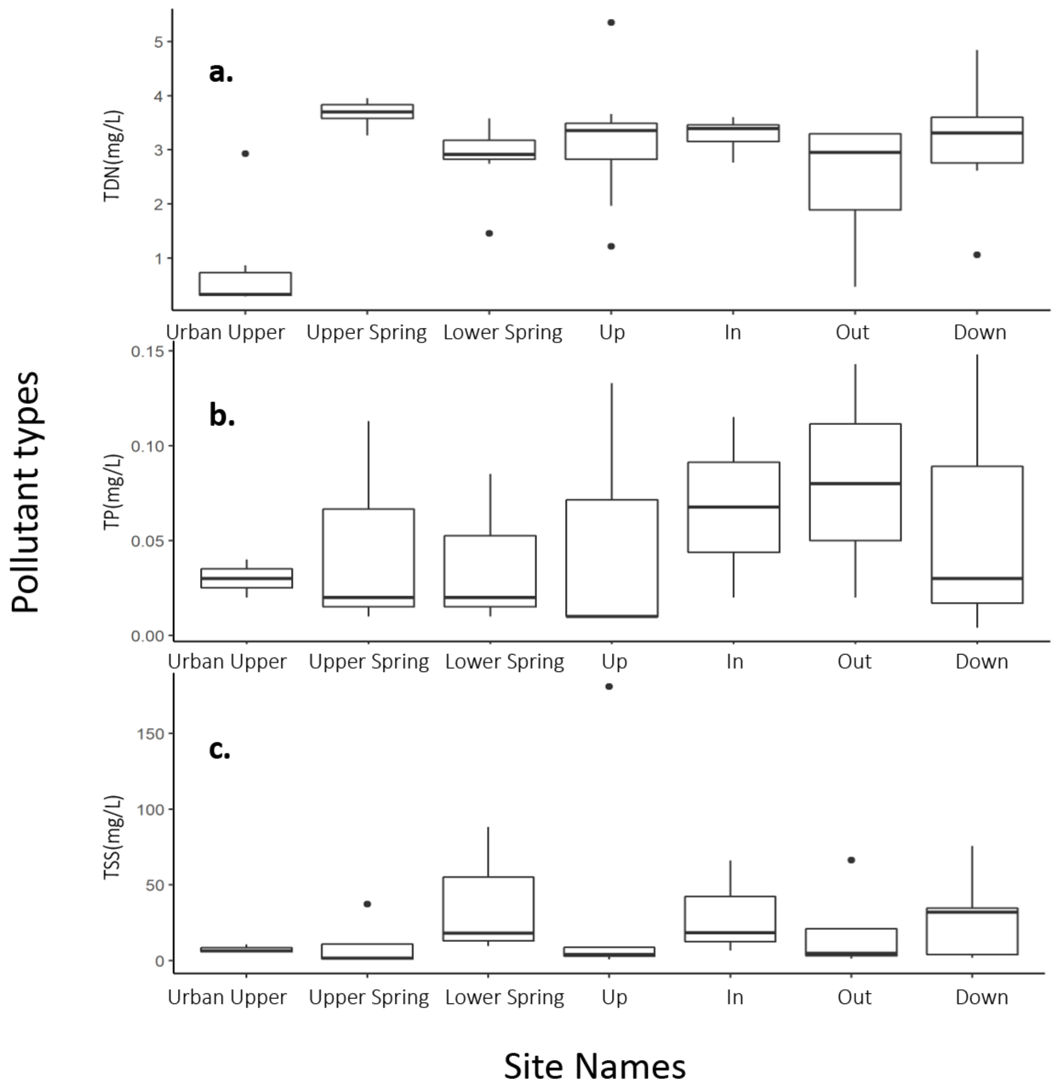

Figure 8 Baseflow concentration of a. TDN, b. TP, c. TSS for each site

Water Discharge During Storm Events

During the monitored period, the stream experienced 52 storm events. In general, the stream exhibited a very flashy response, where rise and fall rates around storm events were rapid. Due to regional drought, water was not able to be diverted into the wetland during most periods between storm events during the monitored period. However, during storm events wetland inflow water levels rapidly increased and maintained for several hours to days, depending on the duration and magnitude of the storm event. Wetland water levels receded well after stream levels did (**Figure 9**).

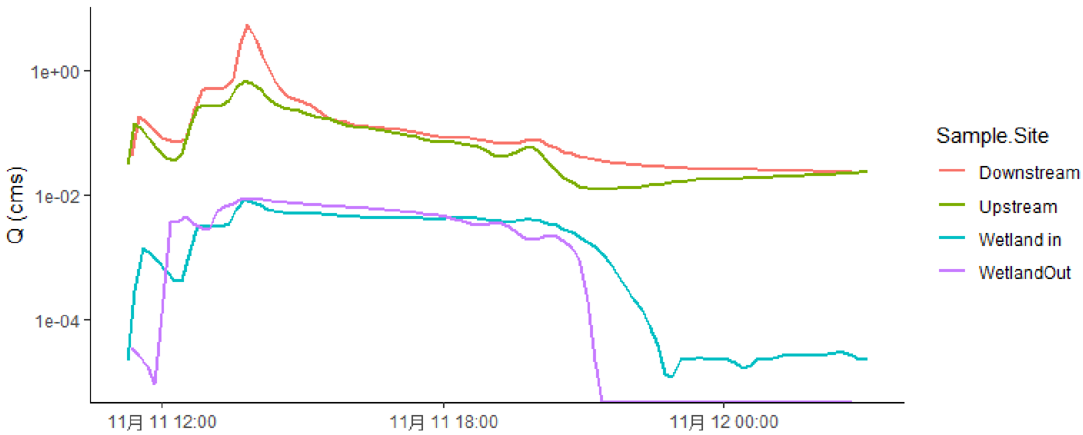

Figure 9 Example water discharge timeseries in storm event of 11/11/2020

Water Wetland Diversion Ratio

Comparison of the volume of runoff diverted into the wetland as compared to the volume of water passing through the stream in a given event revealed that the wetland is able to treat 0.1to 14 % of streamflow (**Figure 10**). The amount of streamflow that is able to be diverted into the wetland is related to the magnitude and intensity of the precipitation event. There is a significant negative correlation between the precipitation intensity and the wetland inflow ratio (**Table 1**). There is a significant positive correlation between the wetland inflow ratio and time duration ratio. There's no significant correlation between wetland inflow ratio and precipitation depth, stream duration and wetland duration.

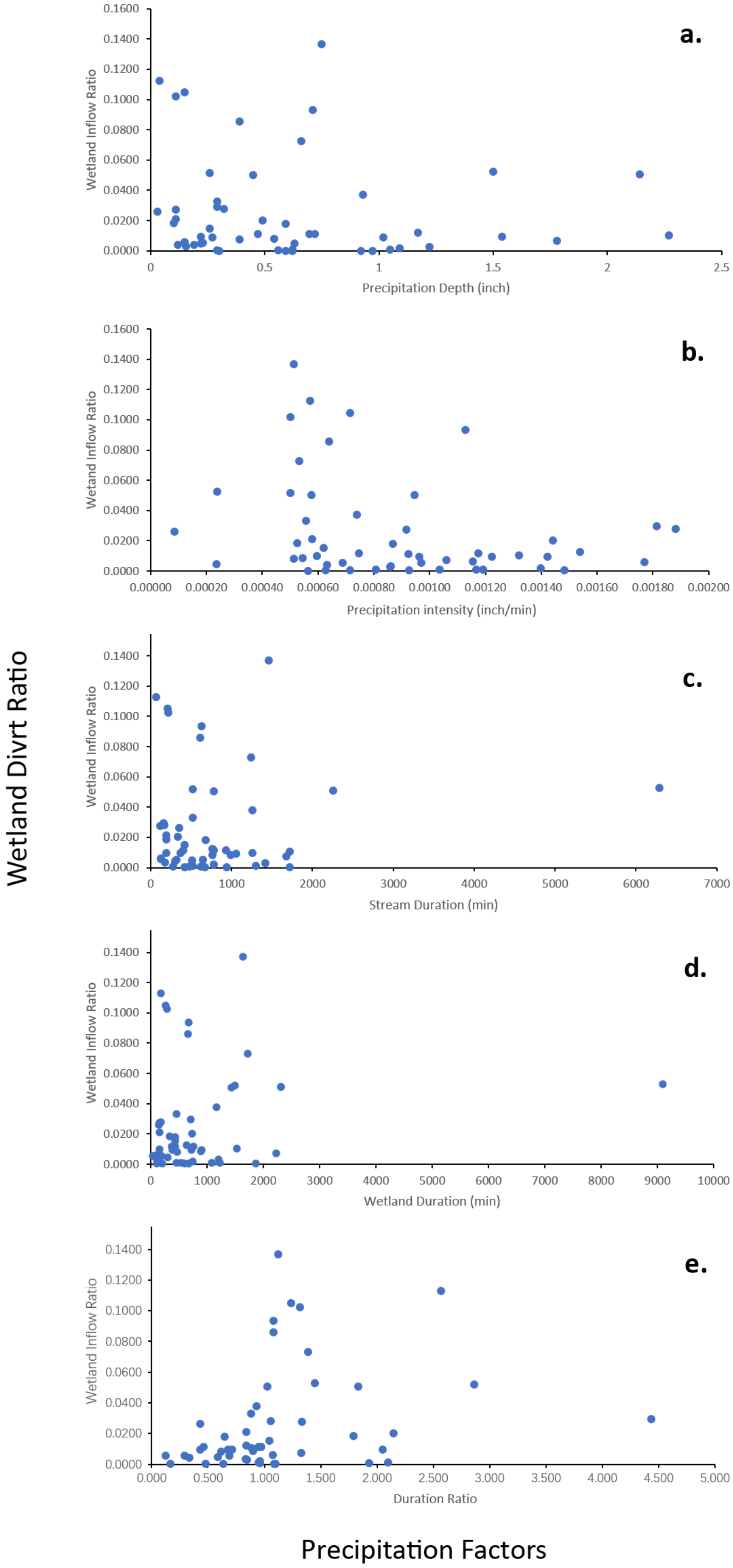

Figure 10. Wetland water diversion ratio and precipitation event factors—a. precipitation depth, .b. precipitation intensity, c. stream event time duration, d. wetland event time duration, e. duration ratio (wetland event duration: stream event duration)

		Precipitation depth	Precipitation intensity	Stream duration	Wetland duration	Duration ratio
Wetland inflow ratio	Pearson Correlation	-0.107	*-0.285	0.091	0.172	*0.297
	Significance (Two Tail)	0.448	0.04	0.52	0.222	0.033
	N	52	52	52	52	52

Table 1. Correlation between wetland water inflow ratio and precipitation event factors
*The correlation is significant at 0.05 level (two-tail)

Pollutants Change at Wetland During Storm Events

During storm events, TDN demonstrated a dilution pattern, where TDN concentrations quickly dropped at the start of the storm, and slowly increased as the hydrograph receded (**Figure 11a.**). On the contrary, TP and TSS demonstrated flushing patterns where concentrations rapidly increased and remained high through the storm, receding with the hydrograph fall (**Figure 11b.** and **c.**). There are significant pollutant load reduction in wetland ('outflow' compare to 'inflow') but no significant pollutant load reduction in stream ('upstream' compare to 'downstream') (**Figure 12**).

Overall, the wetland demonstrated consistent mass reductions in TP and TSS, with TP ranging from -11 to -91 % and TSS ranging from -28 to -99 % (**Table 2**). Nitrogen reductions during storm events were less consistent, with one event having a net gain in TDN at the wetland outlet, and others ranging from -16 to -47% load reductions. There are also 17 to 57% water volume reductions in each event, which demonstrates the wetland has function of stormwater runoff removal.

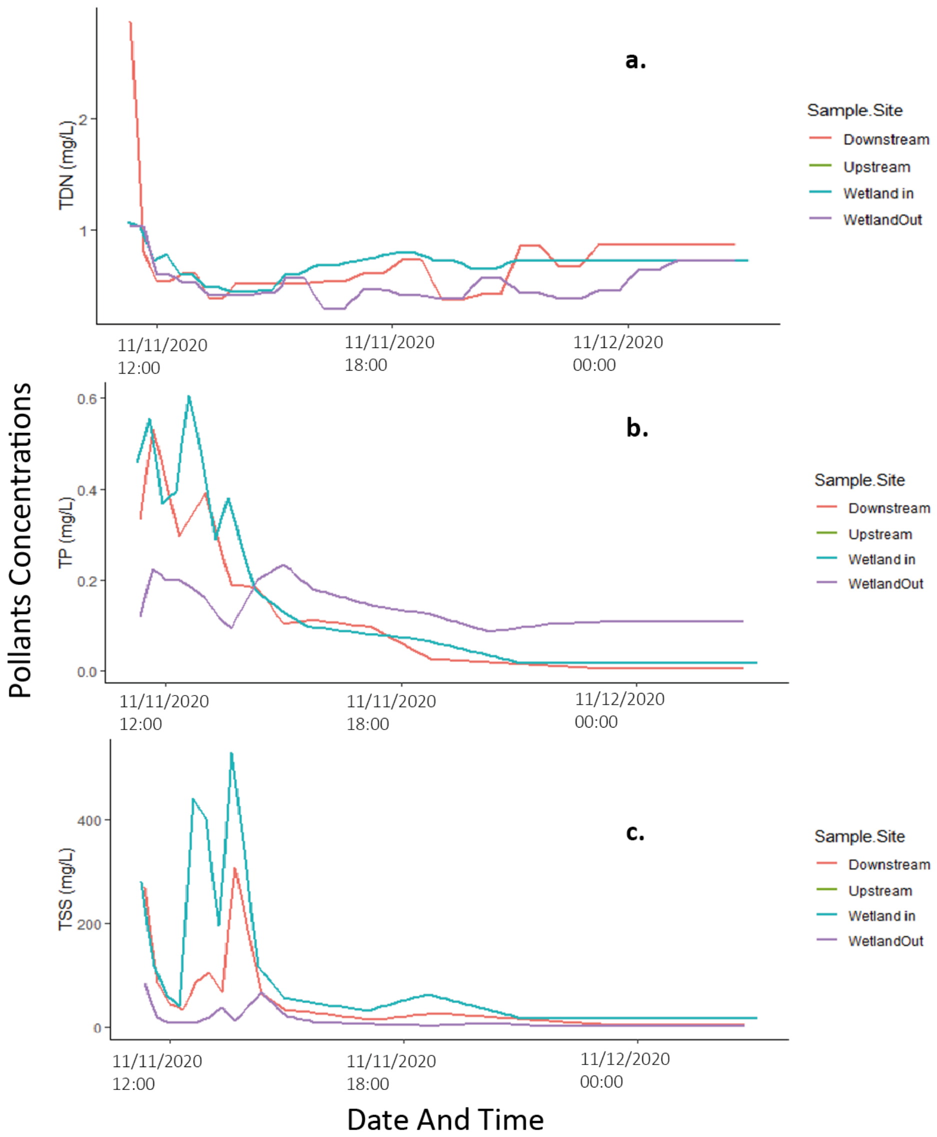

Figure 11. Patterns of a. TDN, b. TP and c. TSS concentrations throughout the November 2020 storm event

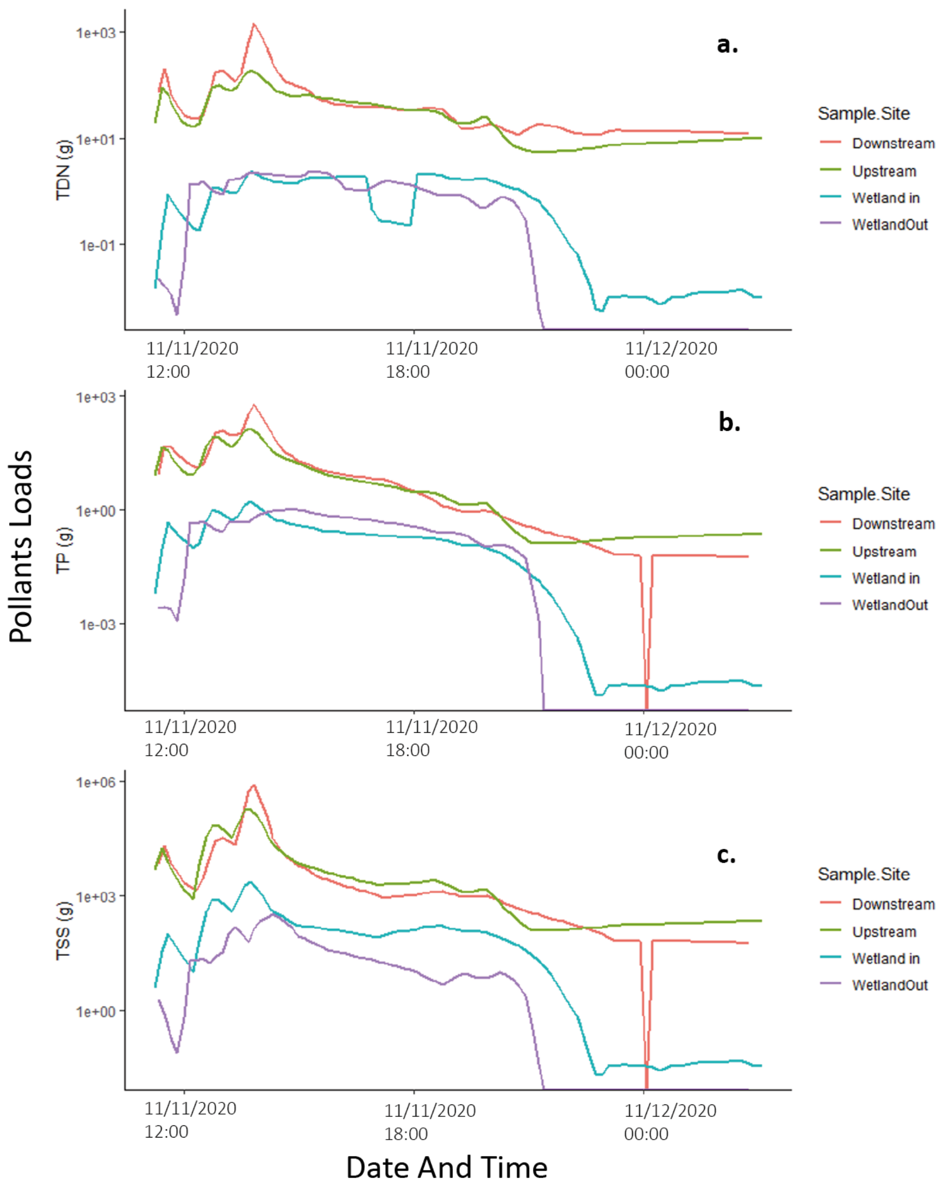

Figure 12. Patterns of a. TDN, b. TP and c. TSS loads throughout the November 2020 storm event

	Volume (%)	TDN (%)	TP (%)	TSS (%)	Avg Flow Rate (m^3/min)
7/9/2020 Storm	-56.78	16.32	-39.15	-47.65	6.38
9/2/2020 Storm	-56.84	-16.00	-91.31	-99.81	7.93
11/11/2020 Storm	-16.96	-32.64	-11.02	-83.09	17.88
3/18/2021 Storm	-40.70	-47.44	-58.10	-28.06	52.02

Table 2. Percentage change of volume and pollutants load comparing outflow to inflow in each captured storm event

Discussions

Pollutant Sources

Synoptic sampling during baseflow times demonstrates high contribution of TDN from the two groundwater springs that enter Walnut Run after it daylights in the park. These springs are likely high in TDN from the legacy of agriculture and associated fertilizer application in the region. Storm events sampled in the stream demonstrate dilution patterns in TDN at the upstream and downstream points (**Figure 11a.**), due to the lower concentration contributions from the urban stormwater inputs. This has implications for when the wetland is most effective, given that highest TDN concentrations occur during lower flow periods.

TP and TSS concentrations are consistently low in the stream and springs during baseflow periods (**Figure 8b., c.**) compared to storm event periods (**Figure 11b., c.**). During storm events, there are initial spikes observed at the stream sampling sites for both of these pollutants at the same time of discharge increase, indicating flushing of these pollutants and that the urban stormwater is a major contributor. It is unclear from the scope of this work whether the sediment and associated phosphorus came primarily from sources up in the watershed, or from scour of the stream banks and bed. Regardless, these patterns during storm events indicate a particularly critical time for attempting to retain incoming phosphorus and sediment.

Baseflow versus Storm Event Patterns in the Wetland

Baseflow synoptic sampling results shows there is an increase in TP (**Figure.8.b.**) concentrations in wetland ('in' and 'out') compared to other sites. TSS also indicates a slight increase at the wetland inflow relative to the upstream sampling point, just several meters away. This could indicate some inaccuracy in the way samples were retrieved and/or that some sediment (and associated phosphorus) is being re-mobilized upon entry of water to the wetland., TDN (**Figure.8.a.**) and TSS concentrations (**Figure.8.c.**) in the wetland decreased between the inflow and outflow (3.4 mg/L on average for inflow and 2.9 mg/L on average for outflow TDN, 20 mg/L for inflow and 4 mg/L for outflow TSS), indicating some retention and removal of these pollutants during baseflow condition. Baseflow discharge measurement shows an average of 0.0015m^3/s discharge in inflow and 0.0009m^3/s in outflow when there is measurable discharge (**Appendix B**). Multiply by average storm event time duration in wetland (**Appendix C**)—845 minutes, we can get:

$$\left(\frac{3.4mg}{L}*\frac{0.0015m^3}{s}-\frac{2.9mg}{L}*\frac{0.0009m^3}{s}\right)*\left(845\text{min}*\frac{60\text{s}}{\text{min}}*\frac{1000\text{L}}{m^3}*\frac{0.001g}{mg}\right)$$
$$=126.24g \quad (7)$$

$$\left(\frac{20mg}{L}*\frac{0.0015m^3}{s}-\frac{4mg}{L}*\frac{0.0009m^3}{s}\right)*\left(845\min*\frac{60s}{\min}*\frac{1000\mathrm{L}}{m^3}*\frac{0.001g}{mg}\right)$$
$$= 1338.48g \quad (8)$$

Therefore, it is estimated that within 845 minutes, 126.24g TDN is removed (7) during baseflow time, and 1338.48g TSS (8) is removed during baseflow time. TDN mass removal in baseflow time is larger than all the TDN mass removal in captured storm events (**Appendix D**). TSS mass removal in baseflow time is comparable to TSS removal in most storm events. That indicates there are significant removal of TDN and TSS during baseflow time provided there is water flow into the wetland. However, our discharge records shows that there is 0 discharge during most baseflow time.

Correspondingly, Table 1 indicates the wetland has high removal efficiency for TSS, good removal efficiency for TP, and relatively low removal efficiency for TDN during storm events. The removal efficiency for each pollutant is related to flushing patterns and retention mechanisms. TSS and TP demonstrate flushing patterns in the stream during storm events, and given that phosphorus is often associated with sediments (Gao et al., 2019; *WQ-10*, 1990), both are retained primarily through physical settling and physio-chemical filtering processes. These patterns aligned to result in the wetland having high removal of TSS and TP loads during storm events. TDN demonstrated dilution during high-flow times (Zhang, 2018). Key retention mechanisms for nitrogen are the biological removal processes of plant uptake and denitrification, both of which depend on adequate residence time for biological interactions. Thus the lower TDN concentrations combined with high flow rates and low residence times led to lower TDN removal efficiencies in the wetland.

The nutrient limitation type in Walnut Run is P-limitation during baseflow times and N-limitation during storm events according to TDN: TP concentration ratio in baseflow times (**Figure 8 a., b.**) and in storm events (**Figure 11 a., b.**). P-limitation is defined as TDN: TP concentration ratio larger than 16, N-limitation is when the ratio smaller than 16 (Gao et al., 2019; Zhang et al., 2021). The wetland shows good capacity in removing excessive TP during N-limitation time, good TDN removal efficiency P-limitation time provided that there is enough water enter into wetland during baseflow time. The mainstream of Chesapeake Bay has N-limitation from June to November each year due to low precipitation and low freshwater input, while P-limitation occurs in other months (Team, 2021; Zhang et al., 2021). Specific to pollutant removal results in each storm event (**Table 1**), the wetland has good TDN removal efficiency in 3/18 event, which is P-limitation time and extraordinary TP removal in some of events (9/12 event) during N-limitation time. Therefore, the wetland is effective in removing the more abundant type of pollutant in Walnut Spring and in Chesapeake Bay.

Comparison of Pollutants Removal Efficiency in Walnut Wetland and Other BMPs

We can compare Walnut Wetland performance with a constructed floodplain wetland that has high similarity. The wetland that located in floodplain of Opequon Creek, Virginia is also a part of Chesapeake Bay watershed, and its main water source comes from urban stormwater and agriculture land (A. Ludwig et al., 2016). It has best load removal efficiencies for TSS (73% in fall and 69.7% in Spring), good removal efficiencies for TP (37% in fall and 24.5% in Spring) and decent removal efficiencies for TDN (16.2 % in fall and 21.5% in Spring). There are better performance for TP, TSS in fall while better performance for TDN in spring (A. Ludwig et al., 2016), which are all same as Walnut Wetland and thus can corroborate our findings.

As N-limitation is becoming a prevail nutrient status in Chesapeake Bay, phosphorous is a more important nutrient to be investigated than nitrogen. (A. L. Ludwig, 2010) summarizes TP removal efficiencies and concentrations in multiple types of constructed wetlands and multiple studies. TP load removal efficiency in Walnut Wetland (11%-91%, 49.8% on average) is slightly lower than floodplain wetlands (30%~80%, 55% on average), moderately higher than urban storm water (15%~70%, 40% on average) and agricultural wetlands (-100%~84%, 30% on average), significantly lower than natural riparian wetlands (mostly 80%~100%).Natural wetlands have best plants, microorganisms and river bed conditions for pollutants assimilation, and all constructed wetlands are trying to simulate natural conditions. Wetlands that located at agriculture land and urban area has heavy pollutant disposal burden and can hardly to simulate nature conditions, thus have low removal efficiency. Floodplains have similar natural conditions as riparian, but it has higher flow rate and lower hydraulic retention time, so the nutrients removal efficiencies are lower. TP concentrations in Walnut Run (0.01-0.6mg/L) and Opequon Creek (0.06 mg/L) are significantly lower than floodplain wetlands listed in (A. L. Ludwig, 2010), which may leads to their lower removal efficiency, as there should be a certain lower limit of effluent TP concentration that can't be treated.

Comparing to other types of BMPs, Walnut Wetland and the wetland in Opequon Creek has lower load removal efficiency of TDN than green roofs (mostly >75%), higher TDN, TP, TSS load removal efficiency than dry detention basin (-50~50%) and similar efficiency as bioretention systems (Liu et al., 2017). Walnut Wetland also has runoff reduction function (17~57%) that only exist in green roofs (48~97%) and permeable pavement (39~97%). That indicate constructed floodplain wetlands as a BMP in Chesapeake Bay is a competitive approach for pollutants and runoff reductions.

Additional influences on wetland performance

The determining factors of TDN and TP removal efficiency are different. Wetland TDN removal efficiency is decided by reaction rate difference between denitrification and nitrification, while denitrification and nitrification rate are decided by wetland temperature. Equations (7)-(9) are expressions for concentration change of TDN in wetlands (Dauda Ahmed et al., 2021). c_e= outflow TDN (mg/L); c_i=inflow TDN concentration (mg/L); K_D= reaction rate constant for denitrification (/d); K_N= reaction rate constant for nitrification (/d); t=hydraulic residence time (d); T_w=wetland ambient temperature (°C).

$$\frac{c_e}{c_i} = e^{-K_N t} + e^{K_D t} - e^{K_N t} e^{K_D t} \quad (9)$$

$$K_D = -(1.048)^{T_w - 20} \quad (10)$$

$$K_N = -0.2187 * (1.048)^{T_w - 20} \quad (11)$$

We can calculate ratio of outflow concentration to inflow concentration ($\frac{c_e}{c_i}$) by substitute $(10), (11)$ into (9) providing the information of hydraulic residence time (t) and wetland ambient temperature (T_w).

$$\frac{c_e}{c_i} = e^{\frac{k_l}{h_l}} \quad (12)$$

$$h_l = \frac{Q_{w-i}}{A_w} \quad (13)$$

TP removal efficiency is decided by hydraulic loading rate (h_l) (m/d) and reaction rate for TP (k_l=-0.0273m/d) (12), while hydraulic loading rate is decided by inflow rate Q_{w-i} (m^3/d) and area of wetland A_w (m^2) (Dauda Ahmed et al., 2021). Substitute (13) into (12), we get:

$$\frac{c_e}{c_i} = e^{\frac{k_l Q_{w-i}}{A_w}} \quad (14)$$

As the area of wetland is regarded as constant, the only variable in $(14)$is Q_{w-i}. Increasing Q_{w-i} results in increasing $\frac{c_e}{c_i}$.

Therefore, there is negative relationship between flow rate and TP removal rate. Average flow rate in a storm event is determined by:

$$Average\ Flow\ Rate = \frac{Total\ volume\ in\ downstream/m^3}{\text{time period of event in downstream/min}} \quad (15)$$

For the storm events in **Table 2**, there is a good fitness that the highest TP removal ratio (91.3%) corresponds to a low flow rate (7.93),the lowest TP removal ratio (11%) corresponds to a high flow rate (17.88),

The difference in TDN and TP concentration removal equations can be explained by difference of TDN and TP removal mechanisms. TDN removal is mainly through nitrification and denitrification facilitated by Dissolved Organic Carbons (DOCs) in wetlands (A. L. Ludwig & Hession, 2015). DOCs are more active in high temperature environments and have better interaction with nitrogen when water stays in wetlands for a longer time. There are significantly more DOCs in spring compare to other seasons (Shatilla & Carey, 2019), which explains the reason for lowest temperature but highest TDN mass removal rate for 3/18/2021 Storm.

TP is mainly removed by fixation with metals and sedimentation (A. L. Ludwig & Hession, 2015), so its removal efficiency is less related with temperature and time of water stays in wetland, but more related with flow rate. Slower flow rate brings better settling and sedimentation, and makes higher removal efficiency of TP.

Future research should apply tracers to more directly study the range of residence times in the wetland, in conjunction with further study of nutrient removal processes.

Percent of streamflow treated by wetland

From the wetland inflow ratio graphs (**Figure 10**), less than 2% of the volume of water in the stream would enter into and be treated by the wetland in most storm events. That means the function of the Walnut Run constructed wetland is limited. Though the wetland is able to efficiently reduce nutrient and sediment loads for the water that is able to enter, the low proportion of water diverted from the stream means the impact on downstream water quality is limited.

The correlation results indicate the wetland inflow ratio has a strong negative relationship with precipitation rate and strong positive relationship with period ratio of wetland event period to stream event period. That means smaller intensity and higher ratio of storm event time in the wetland compared to storm event time in the stream are directly related to a higher ratio of water entering into the wetland.

While precipitation intensity cannot be controlled, design decisions can impact the volume of water diverted and the residence time of water in the wetland. Inlet design as well as wetland depth and volumetric capacity all influence the amount of water treated and residence time of water. The analysis of diverted water volume indicates that the wetland is undersized, but there is not likely an opportunity to modify the sizing. However, modifications to wetland inlet design and management could be made to improve pollutant removal efficiency. In general, presence of multiple entry gates and a flow control valve can help control flow rate fluctuation and allow adequate water to enter in order to make the wetland functioning steadily (Dauda Ahmed et al., 2021). In this case, there are two entry points from the stream, and a control box. The main opportunity to control volume entering from the stream is the wooden weir entry point (**Figure 3**, left). While the wooden slats are designed to be removed to control the level at which water can enter from the stream, the Borough keeps all slats intact, thus minimizing the ability of water to enter the wetland through this inlet location until reaching very high levels. While future modification of this inlet could allow more water to enter the wetland and be treated, it is important to consider that facilitating greater inflows could decrease residence time and impact pollutant removal efficiency.

Conclusions

Pollutants are general concerns in Chesapeake Bay. Constructed wetland is an effective BMP in removing nitrogen, phosphorous and sediments, which is not being sufficiently investigated. There is a constructed floodplain wetland located in State College, Pennsylvania in Chesapeake Bay Watershed called Walnut Wetland. This thesis research has investigated the function of Walnut Wetland including its hydrology, and nitrogen, phosphorus, and sediment patterns from baseflow and stormwater samples from multiple sites in the wetland and adjacent urban stream. The data has demonstrated that the wetland provides significant reduction in nitrogen when it receives water during baseflow time due to high nitrogen inputs from spring-fed streamflow, but relatively low removal efficiency (-16~47 %) during storm events due to its diluting pattern and short residence time. Sediment (28~99%) and phosphorus (11%~91%) removal ratios in the wetland are high because of their flushing patterns and that the wetland facilitates settling and filtering. The wetland has good nitrogen removal efficiency during P-limitation time and good Phosphorous removal efficiency during N-limitation time. The wetland also has the function of stormwater runoff removal (17~57%). While the constructed floodplain wetland has high water quality performance when examining the wetland itself, its impact on the stream is limited due to the amount of water diverted from the stream to the wetland being only between 1~5% of streamflow. Future research can explore possible design and management interventions, such as inlet redesign, to increase the impact of the wetland on downstream water quality especially during baseflow time.

References

Ator, S. W., García, A. M., Schwarz, G. E., Blomquist, J. D., & Sekellick, A. J. (2019). Toward Explaining Nitrogen and Phosphorus Trends in Chesapeake Bay Tributaries, 1992–2012. *JAWRA Journal of the American Water Resources Association*, *55*(5), 1149–1168. https://doi.org/10.1111/1752-1688.12756

Birch, G. F., Matthai, C., Fazeli, M. S., & Suh, J. Y. (2004). Efficiency of a constructed wetland in removing contaminants from stormwater. *Wetlands*, *24*(2), 459–466. https://doi.org/10.1672/0277-5212(2004)024[0459:EOACWI]2.0.CO;2

Campbell, P. C., Bash, J. O., Nolte, C. G., Spero, T. L., Cooter, E. J., Hinson, K., & Linker, L. C. (2019). Projections of Atmospheric Nitrogen Deposition to the Chesapeake Bay Watershed. *Journal of Geophysical Research: Biogeosciences*, *124*(11), 3307–3326. https://doi.org/10.1029/2019JG005203

Clary, J., Jones, J., Leisenring, M., Hobson, P., & Strecker, E. (2020). *International Stormwater BMP Database: 2020 Summary Statistics*. 118.

Dauda Ahmed, S., Kwaku Agodzo, S., & Amaning Adjei, K. (2021). Designing River Diversion Constructed Wetland for Water Quality Improvement. In A. Devlin, J. Pan, & M. Manjur Shah (Eds.), *Inland Waters—Dynamics and Ecology*. IntechOpen. https://doi.org/10.5772/intechopen.92119

Davis, B. J. K., Jacobs, J. M., Davis, M. F., Schwab, K. J., DePaola, A., & Curriero, F. C. (2017). Environmental Determinants of Vibrio parahaemolyticus in the Chesapeake Bay. *Applied and Environmental Microbiology*, *83*(21).

https://doi.org/10.1128/AEM.01147-17

DeLuca, N. M., Zaitchik, B. F., & Curriero, F. C. (2018). Can Multispectral Information Improve Remotely Sensed Estimates of Total Suspended Solids? A Statistical Study in Chesapeake Bay. *Remote Sensing*, *10*(9), 1393. https://doi.org/10.3390/rs10091393

Dodds, W., & Smith, V. (2016). Nitrogen, phosphorus, and eutrophication in streams. *Inland Waters*, *6*(2), 155–164. https://doi.org/10.5268/IW-6.2.909

Facts & Figures | Chesapeake Bay Program. (2017). https://www.chesapeakebay.net/discover/facts

Fanelli, R. M., Blomquist, J. D., & Hirsch, R. M. (2019). Point sources and agricultural practices control spatial-temporal patterns of orthophosphate in tributaries to Chesapeake Bay. *Science of The Total Environment*, *652*, 422–433. https://doi.org/10.1016/j.scitotenv.2018.10.062

Foladori, P., Petrini, S., & Andreottola, G. (2020). How suspended solids concentration affects nitrification rate in microalgal-bacterial photobioreactors without external aeration. *Heliyon*, *6*(1), e03088. https://doi.org/10.1016/j.heliyon.2019.e03088

Gao, Y., Jia, Y., Yu, G., He, N., Zhang, L., Zhu, B., & Wang, Y. (2019). Anthropogenic reactive nitrogen deposition and associated nutrient limitation effect on gross primary productivity in inland water of China. *Journal of Cleaner Production*, *208*, 530–540. https://doi.org/10.1016/j.jclepro.2018.10.137

Harding, L. W., Mallonee, M. E., Perry, E. S., David Miller, W., Adolf, J. E., Gallegos, C. L., & Paerl, H. W. (2020). Seasonal to Inter-Annual Variability of Primary Production in Chesapeake Bay: Prospects to Reverse Eutrophication and Change Trophic

Classification. *Scientific Reports*, *10*(1), 2019. https://doi.org/10.1038/s41598-020-58702-3

How Streamflow is Measured. (2021). https://www.usgs.gov/special-topic/water-science-school/science/how-streamflow-measured?qt-science_center_objects=0#qt-science_center_objects

Keddy, P. A. (2010). *Wetland Ecology: Principles and Conservation*. Cambridge University Press.

Keeter, B. (2019, February 20). *Floodplains and Wetlands* [Text]. NASA. http://www.nasa.gov/emd/nrm-floodplains-and-wetlands

Liu, Y., Engel, B. A., Flanagan, D. C., Gitau, M. W., McMillan, S. K., & Chaubey, I. (2017). A review on effectiveness of best management practices in improving hydrology and water quality: Needs and opportunities. *Science of The Total Environment*, *601–602*, 580–593. https://doi.org/10.1016/j.scitotenv.2017.05.212

Ludwig, A., Hession, W. C., Scott, D., & Gallagher, D. (2016). Simulated Flood of a Small Constructed Floodplain Wetland in Virginia: Event-Scale Pollutant Attenuation. *Transactions of the ASABE*, *59*(5), 1319–1329. https://doi.org/10.13031/trans.59.11622

Ludwig, A. L. (2010). *Constructed Floodplain Wetland Effectiveness for Stormwater Management*. 191.

Ludwig, A. L., & Hession, W. C. (2015). Groundwater influence on water budget of a small constructed floodplain wetland in the Ridge and Valley of Virginia, USA. *Journal of Hydrology: Regional Studies*, *4*, 699–712. https://doi.org/10.1016/j.ejrh.2015.10.003

O'Shea, M. L., Borst, M., Liao, D., Yu, S. L., & Earles, T. A. (1999). Constructed Wetlands for Stormwater Management. *WRPMD'99*, 1–11. https://doi.org/10.1061/40430(1999)158

Pennsylvania's Blueprint for Clean Water. (2021). https://www.cbf.org/how-we-save-the-bay/chesapeake-clean-water-blueprint/2020-state-of-the-blueprint/pennsylvanias-2020-blueprint-for-clean-water.html

Resende, J. D., Nolasco, M. A., & Pacca, S. A. (2019). Life cycle assessment and costing of wastewater treatment systems coupled to constructed wetlands. *Resources, Conservation and Recycling*, *148*, 170–177. https://doi.org/10.1016/j.resconrec.2019.04.034

Run, T. (n.d.). *Water Resource Publication*. 62.

Section 4. Sources of Nitrogen, Phosphorus and Sediment to the Chesapeake Bay. (2010). 44.

Shatilla, N. J., & Carey, S. K. (2019). Assessing inter-annual and seasonal patterns of DOC and DOM quality across a complex alpine watershed underlain by discontinuous permafrost in Yukon, Canada. *Hydrology and Earth System Sciences*, *23*(9), 3571–3591. https://doi.org/10.5194/hess-23-3571-2019

Shenk, G. W., & Linker, L. C. (2013). Development and Application of the 2010 Chesapeake Bay Watershed Total Maximum Daily Load Model. *JAWRA Journal of the American Water Resources Association*, *49*(5), 1042–1056. https://doi.org/10.1111/jawr.12109

Son, S., & Wang, M. (2012). Water properties in Chesapeake Bay from MODIS-Aqua measurements. *Remote Sensing of Environment*, *123*, 163–174. https://doi.org/10.1016/j.rse.2012.03.009

Steidinger, B. S., Turner, B. L., Corrales, A., & Dalling, J. W. (2015). Variability in potential to exploit different soil organic phosphorus compounds among tropical montane tree species. *Functional Ecology*, *29*(1), 121–130. https://doi.org/10.1111/1365-2435.12325

Team, N. W. S. C. I. W. (n.d.). *Climate Information—National Weather Service Central PA*. Retrieved June 5, 2021, from https://w2.weather.gov/climate/xmacis.php?wfo=ctp

Team, N. W. S. C. I. W. (2021). *Climate Information—National Weather Service Central PA*. Climate Information - National Weather Service Central PA. https://w2.weather.gov/climate/xmacis.php?wfo=ctp

Testa, J. M., Clark, J. B., Dennison, W. C., Donovan, E. C., Fisher, A. W., Ni, W., Parker, M., Scavia, D., Spitzer, S. E., Waldrop, A. M., Vargas, V. M. D., & Ziegler, G. (2017). Ecological Forecasting and the Science of Hypoxia in Chesapeake Bay. *BioScience*, *67*(7), 614–626. https://doi.org/10.1093/biosci/bix048

Tian, R. (2020). Factors Controlling Hypoxia Occurrence in Estuaries, Chester River, Chesapeake Bay. *Water*, *12*(7), 1961. https://doi.org/10.3390/w12071961

Total Nitrogen in Wastewater. (n.d.). CHEMSCAN. Retrieved May 28, 2021, from https://www.chemscan.com/total-nitrogen-in-wastewater.html

US EPA, O. (2013, March 12). *The Effects* [Collections and Lists]. US EPA. https://www.epa.gov/nutrientpollution/effects

Vymazal, J. (2010). Constructed Wetlands for Wastewater Treatment. *Water*, *2*(3), 530–549. https://doi.org/10.3390/w2030530

WQ-10. (1990). https://www.extension.purdue.edu/extmedia/wq/wq-10.html

Xu, C., Hong, J., Jia, H., Liang, S., & Xu, T. (2017). Life cycle environmental and economic assessment of a LID-BMP treatment train system: A case study in China. *Journal of Cleaner Production*, *149*, 227–237. https://doi.org/10.1016/j.jclepro.2017.02.086

Yin, S., Bai, J., Wang, W., Zhang, G., Jia, J., Cui, B., & Liu, X. (2019). Effects of soil moisture on carbon mineralization in floodplain wetlands with different flooding frequencies. *Journal of Hydrology*, *574*, 1074–1084. https://doi.org/10.1016/j.jhydrol.2019.05.007

Zhang, Q. (2018). Synthesis of nutrient and sediment export patterns in the Chesapeake Bay watershed: Complex and non-stationary concentration-discharge relationships. *Science of The Total Environment*, *618*, 1268–1283. https://doi.org/10.1016/j.scitotenv.2017.09.221

Zhang, Q., Fisher, T. R., Trentacoste, E. M., Buchanan, C., Gustafson, A. B., Karrh, R., Murphy, R. R., Keisman, J., Wu, C., Tian, R., Testa, J. M., & Tango, P. J. (2021). Nutrient limitation of phytoplankton in Chesapeake Bay: Development of an empirical approach for water-quality management. *Water Research*, *188*, 116407. https://doi.org/10.1016/j.watres.2020.116407

Appendices

Appendix A--R code for Baseflow separation

```
# Set up necessary libraries
library(dplyr)
library(plyr)
library(stringr)
library(EcoHydRology)  #for  calculating  various ecohydrologic metrics,  including  doing hydrograph separation
library(dygraphs) #for making interactive plots
library(zoo) #for formatting data for interactive plot
  ## Get an approximation for baseflow using a 3 pass filter:
 bfs<-BaseflowSeparation(streamdata$Q_cms, passes=3)

  #add the dataframe of baseflow to the original dataframe by combining columns (cbind)
 streamdata=cbind(streamdata,bfs)

#Initialize variables
Qdiffsum=rep(0, length(streamdata$Q_cms))
Qtotal=rep(0, length(streamdata$Q_cms))
Qdiff=rep(0, length(streamdata$Q_cms))

#specify sample interval
sampleint_min=10
sampleint_s=sampleint_min*60

#conversion for m3 to liters
m3ToL= 1000

# Set up loop to calculate index
#   calculate values for entire record length
# for(d in 2:length(streamdata$Qcfs)){
#   Qdiff[d]=abs(streamdata$Qcfs[d]-streamdata$Qcfs[d-1])
#   Qdiffsum[d]=Qdiffsum[d-1]+Qdiff[d]
#   Qtotal[d]=Qtotal[d-1]+streamdata$Qcfs[d]
# }
#
# RB=Qdiffsum[length(streamdata$Qcfs)]/Qtotal[length(streamdata$Qcfs)]
# CVD= sd(streamdata$Qcfs)/mean(streamdata$Qcfs)

# calculate values for each year
```

```
numYears=(as.numeric(maxYear)-as.numeric(minYear))+1
RB_allyrs = as.data.frame(matrix(nrow = numYears, ncol = 2))
colnames(RB_allyrs)=c("Year","RB")
CVD_allyrs=as.data.frame(matrix(nrow = numYears, ncol = 2))
colnames(CVD_allyrs)=c("Year","CVD")

#for selected time frame, looping through Q data to calculate R-B flashiness index

  Qdiffsum=rep(0, length(streamdata_yr$Q_cms))
  Qtotal=rep(0, length(streamdata_yr$Q_cms))
  Qdiff=rep(0, length(streamdata_yr$Q_cms))

   for(i in 2:length(streamdata_yr$Q_cms)){
    Qdiff[i]=abs(streamdata_yr$Q_cms[i]-streamdata_yr$Q_cms[i-1])
    Vol_L[i]=Qdiff[i]*sampleint_s*m3ToL

    Qdiffsum[i]=Qdiffsum[i-1]+Qdiff[i]
    Qtotal[i]=Qtotal[i-1]+streamdata_yr$Q_cms[i]
    Voltotal[i]=Vol_L[i-1]+Vol_L[i]
   }
   #filling in a table with values of average R-B index and coefficient of variation for each water
year
   #If there is no data for a year simply fill in NA
  RB_allyrs[j,1]=YearNum
  CVD_allyrs[j,1]=YearNum
   if(length(streamdata_yr$Q_cms)>1) {
      RB_allyrs[j,2]=Qdiffsum[length(streamdata_yr$Q_cms)]/Qtotal[length(streamdata_yr$Q_c
ms)]
     CVD_allyrs[j,2]=sd(streamdata_yr$Q_cms)/mean(streamdata_yr$Q_cms)
   }

#making new filenames, using part of original name, and saving to two new files with R-B
index and CV
RBfilename=paste(streamdata,"_RB.csv", sep = "")
CVDfilename=paste(streamdata,"_CVD.csv", sep = "")
write.csv(RB_allyrs, file= RBfilename)
write.csv(CVD_allyrs, file= CVDfilename)
```

Appendix B--Baseflow discharge at wetland

Inflow:

DateTime	Staff gage (m)	Sensor Type	Sensor depth (m)	Discharge (cfs)	Discharge (cms)
9/29/20 17:15	NA	HOBO	0.11	0.032	0.00091
3/18/21 17:25		HOBO	0.117	0.072	0.00204

Outflow:

DateTime	Sensor depth (m)	Discharge (cfs)	Discharge (cms)
7/16/2019	0.078	0.05268	0.00149
8/21/2019	0.154	0.05415	0.00153
4/27/2020	0.163	0.01702	0.00048
9/30/2020	0.136	8.2953E-06	2.34897E-07

Appendix C--Storm Events Records (2020.3.1~2021.3.18)

Event satrt date	Total volume in Outlow/m3	Total volume in downstream/m3	Wetland ratio	Precip date	Precip/inch	Event Duration Down/min	Event Duration Out/min	stream intensity	wetland intensity	Period Ratio	precip rate
2020/3/10	14.23	126.08	0.1128	2020/3/11	0.04	70	180	1.801	0.079	2.571	0.00057
2020/3/13	46.49	453.89	0.1024	2020/3/13	0.11	220	290	2.063	0.160	1.318	0.00050
2020/3/18	436.29	4661.73	0.0936	2020/3/19	0.71	630	680	7.400	0.642	1.079	0.00113
2020/3/19	818.84	5977.62	0.1370	3/20-21/2020	0.75	1460	1640	4.094	0.499	1.123	0.00051
2020/3/23	213.46	2484.99	0.0859	2020/3/24	0.39	610	660	4.074	0.323	1.082	0.00064
2020/3/25	60.33	574.32	0.1050	2020/3/26	0.15	210	260	2.735	0.232	1.238	0.00071
2020/3/28	1141.94	22484.27	0.0508	3.28-29/2020	2.14	2260	2320	9.949	0.492	1.027	0.00095
2020/4/8	132.42	11590.32	0.0114	4/8-9/2020	0.72	780	760	14.859	0.174	0.974	0.00092
2020/4/9	56.51	1711.03	0.0330	2020/4/10	0.29	520	460	3.290	0.123	0.885	0.00056

2020/4/17	210.46	5580.61	0.0377	4/18-19/2020	0.93	1260	1170	4.429	0.180	0.929	0.00074
2020/4/26	325.61	4461.66	0.0730	2020/4/27	0.66	1240	1720	3.598	0.189	1.387	0.00053
2020/4/30	1039.62	19683.69	0.0528	4/30/2020-5/3/2020	1.5	6290	9100	3.129	0.114	1.447	0.00024
2020/5/6	134.16	2650.97	0.0506	5/7-8/2020	0.45	780	1430	3.399	0.094	1.833	0.00058
2020/5/8	69.76	1345.05	0.0519	5/8-9/2020	0.26	520	1490	2.587	0.047	2.865	0.00050
2021/5/22	89.04	5898.92	0.0151	2020/5/23	0.26	420	440	14.045	0.202	1.048	0.00062
2020/5/23	19.74	930.18	0.0212	2020/5/24	0.11	190	160	4.896	0.123	0.842	0.00058
2020/5/28	100.45	213978.71	0.0005	2020/5/29	0.92	620	680	345.127	0.148	1.097	0.00148
2020/6/3	16.15	37235.64	0.0004	2020/6/4	0.59	940	600	39.612	0.027	0.638	0.00063
2020/6/4	373.03	1549046.06	0.0002	6/5-6/2020	0.97	1720	1870	900.608	0.199	1.087	0.00056
2020/6/10	217.48	30104.78	0.0072	6/10-12/2020	1.78	1680	2230	17.920	0.098	1.327	0.00106
2020/6/19	45.45	2244.69	0.0202	2020/6/20	0.49	340	730	6.602	0.062	2.147	0.00144
2020/6/22	53.83	54774.90	0.0010	2020/6/23	0.62	520	1090	105.336	0.049	2.096	0.00119

2020/6/25	8.07	437.14	0.0185	2020/6/26	0.1	190	340	2.301	0.024	1.789	0.00053
2020/6/27	23.13	782.37	0.0296	6/27-28/2020	0.29	160	710	4.890	0.033	4.438	0.00181
2020/7/8	11.43	1211.18	0.0094	2020/7/9	0.27	190	390	6.375	0.029	2.053	0.00142
2020/7/19	7.58	1677.85	0.0045	2020/7/20	0.12	510	300	3.290	0.025	0.588	0.00024
2020/7/22	1.86	303.96	0.0061	2020/7/23	0.15	130	140	2.338	0.013	1.077	0.00115
2020/7/24	1.34	233.86	0.0057	2020/7/24	0.23	130	90	1.799	0.015	0.692	0.00177
2020/7/31	32.17	2799.63	0.0115	7/31/2020-8/1/2020	0.47	400	380	6.999	0.085	0.950	0.00118
2020/8/1	7.62	277.42	0.0275	2020/8/2	0.11	120	160	2.312	0.048	1.333	0.00092
2020/8/7	18.32	701.70	0.0261	2020/8/8	0.03	350	150	2.005	0.122	0.429	0.00009
2020/8/25	23.41	836.60	0.0280	2020/8/25	0.32	170	180	4.921	0.130	1.059	0.00188
2020/8/28	104.96	35578.21	0.0030	8/29-30/2020	1.22	1420	1200	25.055	0.087	0.845	0.00086
2020/9/2	66.21	7853.01	0.0084	2020/9/3	0.54	990	890	7.932	0.074	0.899	0.00055
2020/9/29	57.17	5973.95	0.0096	2020/9/30	1.54	1260	900	4.741	0.064	0.714	0.00122

2020/10/12	16.26	3021.54	0.0054	2020/10/12	0.63	650	190	4.649	0.086	0.292	0.00097
2020/10/13	3.04	565.33	0.0054	2020/10/13	0.22	320	40	1.767	0.076	0.125	0.00069
2020/10/29	65.61	7003.16	0.0094	10/29-30/2020	1.02	1060	720	6.607	0.091	0.679	0.00096
2020/10/30	0.68	1487.55	0.0005	10/30-31/2020	0.62	670	110	2.220	0.006	0.164	0.00093
2020/11/1	2.23	530.28	0.0042	2020/11/2	0.19	300	100	1.768	0.022	0.333	0.00063
2020/11/11	168.37	13587.89	0.0124	2020/11/12	1.17	760	640	17.879	0.263	0.842	0.00154
2020/11/15	8.99	926.34	0.0097	2020/11/16	0.22	370	160	2.504	0.056	0.432	0.00059
2020/11/22	48.66	2683.03	0.0181	2020/11/23	0.59	680	440	3.946	0.111	0.647	0.00087
2020/11/25	13.98	1723.31	0.0081	2020/11/26	0.39	760	470	2.268	0.030	0.618	0.00051
2020/11/30	43.03	3740.78	0.0115	2020/11/30-12/1	0.695	930	430	4.022	0.100	0.462	0.00075
2020/12/1	0.85	263.16	0.0032	2020/12/1-2	0.155	180	150	1.462	0.006	0.833	0.00086
2020/12/24	363.55	34785.16	0.0105	2020/12/25-26	2.27	1720	1530	20.224	0.238	0.890	0.00132
2021/1/1	16.39	22145.23	0.0007	2021/1/2	0.56	480	460	46.136	0.036	0.958	0.00117

2021/1/15	4.02	9434.80	0.0004	2021/1/16	0.3	420	200	22.464	0.020	0.476	0.00071
2021/2/28	89.23	91260.46	0.0010	2021/3/1	1.05	1300	1230	70.200	0.073	0.946	0.00081
2021/3/11	8.53	9452.63	0.0009	2021/3/12	0.29	280	540	33.759	0.016	1.929	0.00104
2021/3/18	80.08	40571.45	0.0020	3/18-19/2021	1.09	780	750	52.015	0.107	0.962	0.00140

Appendix D--Pollutants Mass Change Outflow to Inflow

	Total TN _g	Total TP_g	Total TSS_g
7/9/2020 Storm	2.70	-1.37	-481.78
9/2/2020 Storm	-2.70	-31.79	-313214.00
11/11/2020 Storm	-34.91	-3.21	-13940.03
3/18/2021 Storm	-47.93	-10.42	-2316.54